Chemical pressure effects on the spectroscopic properties of Nd^{3+}-doped gallium nano-garnets

V. Monteseguro,[1] M. Rathaiah,[2] K. Linganna,[2] A.D. Lozano-Gorrín,[1] M.A. Hernández-Rodríguez,[1] I.R. Martín,[1] P. Babu,[3] U.R. Rodríguez-Mendoza,[1] F.J. Manjón,[4] A. Muñoz,[1] C.K. Jayasankar,[5] V. Venkatramu[2,6] and V. Lavín[1,7]

[1]*Department of Physics, and MALTA Consolider Team, Universidad de La Laguna, 38200 San Cristóbal de La Laguna, Santa Cruz de Tenerife, Spain*
[2]*Departamento de Física, Yogi Vemana University, Kadapa-516 003, India*
[3]*Department of Physics, Government Degree College, Satyavedu-517 588, India*
[4]*Instituto de Diseño para la Fabricación y Producción Automatizada, and MALTA Consolider Team, Universitat Politécnica de València, 46022 Valencia, Spain*
[5]*Department of Physics, Sri Venkateswara University, Tirupati-517 502, India*
[6]*vvramuphd@gmail.com*
[7]*vlavin@ull.edu.es*

Abstract: Nd^{3+}-doped $RE_3Ga_5O_{12}$ (RE = Gd, Y, and Lu) nano-crystalline garnets of 40-45 nm in size have been synthesized by a sol-gel method. With the decrease of the RE atom size, the chemical pressure related to the decreasing volumes of the GaO_4 tetrahedral, GaO_6 octahedral and REO_8 dodecahedral units drive the nano-garnets toward a more compacted structure, which is evidenced by the change of the vibrational phonon mode frequencies. The chemical pressure also increases the crystal-field strength felt by the RE^{3+} ions while decreases the orthorhombic distortion of the REO_8 local environment. These effects alter the absorption and emission properties of the Nd^{3+} ion measured in the near-infrared luminescence range from 0.87 to 1.43 μm associated with the $^4F_{3/2}\rightarrow{}^4I_J$ (J = 9/2, 11/2, 13/2) transitions. The $^4F_{3/2}$ luminescence decay curves show non-exponential behavior due to dipole-dipole energy transfer interactions among Nd^{3+} ions that increases with pressure.

OCIS codes: (160.4236) Nanomaterials; (140.3530) Lasers, neodymium; (140.3550) Lasers, Raman; (160.4760) Optical properties.

References and links

1. M. J. Weber, "Rare earth lasers," in *Handbook on the Physics and Chemistry of Rare Earths*, K.A. Gschneidner, Jr. and L. Eyring, eds. (North Holland Publishing Company, 1979), vol. 4, ch. 35, p. 275.
2. M. Pollnau, P. J. Hardman, W. A. Clarkson, and D. C. Hanna, "Upconversion, lifetime quenching, and ground-state bleaching in Nd^{3+}:$LiYF_4$," Opt. Commun. **147**(1-3), 203–211 (1998).
3. A. A. Kaminskii, *Laser Crystals* (Springer-Verlag, 1981).
4. C. D. Brandle and R. L. Barns, "Crystal stoichiometry of Czochralski grown rare-earth gallium garnets," J. Cryst. Growth **26**(1), 169–170 (1974).
5. V. Venkatramu, M. Giarola, G. Mariotto, S. Enzo, S. Polizzi, C. K. Jayasankar, F. Piccinelli, M. Bettinelli, and A. Speghini, "Nanocrystalline lanthanide-doped $Lu_3Ga_5O_{12}$ garnets: interesting materials for light-emitting devices," Nanotechnology **21**(17), 175703 (2010).
6. A. Speghini, F. Piccinelli, and M. Bettinelli, "Synthesis, characterization and luminescence spectroscopy of oxide nanopowders activated with trivalent lanthanide ions: The garnet family," Opt. Mater. **33**(3), 247–257 (2011).
7. R. Krsmanović, V. A. Morozov, O. I. Lebedev, S. Polizzi, A. Speghini, M. Bettinelli, and G. Van Tendeloo, "Structural and luminescence investigation on gadolinium gallium garnet nanocrystalline powders prepared by solution combustion synthesis," Nanotechnology **18**(32), 325604 (2007).
8. R. Naccache, F. Vetrone, A. Speghini, M. Bettinelli, and J. A. Capobianco, "Cross relaxation and upconversion processes in Pr^{3+} singly doped and Pr^{3+}/Yb^{3+} codoped nanocrystalline $Gd_3Ga_5O_{12}$: The sensitizer/activator relationship," J. Phys. Chem. C **112**(20), 7750–7756 (2008).

#240253 Received 5 May 2015; revised 23 Jun 2015; accepted 23 Jun 2015; published 2 Jul 2015

9. Th. Tröster, "Optical studies of non-metallic compounds under pressure," in *Handbook on the Physics and Chemistry of Rare Earths*, K.A. Gschneidner, Jr., J.-C. G. Bunzli, and V.K. Pecharsky, eds. (Elsevier Science B.V., 2003) vol. 33, ch. 217, p. 515.
10. E. Antic-Fidancev, J. Hölsa, M. Lastusaari, and A. Lupei, "Dopant-host relationships in rare-earth oxides and garnets doped with trivalent rare-earth ions," Phys. Rev. B **64**(19), 195108 (2001).
11. J. Rodríguez-Carvajal, "Recent advances in magnetic structure determination by neutron powder diffraction," Physica B **192**(1-2), 55–69 (1993).
12. V. Monteseguro, P. Rodríguez-Hernández, H. M. Ortiz, V. Venkatramu, F. J. Manjón, C. K. Jayasankar, V. Lavín, and A. Muñoz, "Structural, elastic and vibrational properties of nanocrystalline lutetium gallium garnet under high pressure," Phys. Chem. Chem. Phys. **17**(14), 9454–9464 (2015).
13. S. Ray, S. F. León-Luis, F. J. Manjón, M. A. Mollar, O. Gomis, U. R. Rodríguez-Mendoza, S. Agouram, A. Muñoz, and V. Lavín, "Broadband, site selective and time resolved photoluminescence spectroscopic studies of finely size-modulated Y_2O_3:Eu^{3+} phosphors synthesized by a complex based precursor solution method," Curr. Appl. Phys. **14**(1), 72–81 (2014).
14. B. G. Wybourne, *Spectroscopic Properties of Rare Earths* (Wiley-Interscience, 1965).
15. C. A. Morrison and R. P. Leavitt, "Spectroscopic properties of triply ionized lanthanides in transparent host crystals," in *Handbook on the Physics and Chemistry of Rare Earths*, edited by K.A. Gschneidener, Jr. and L. Eyring, eds. (North Holland Publishing Company, 1982), vol. 5, ch. 46, p. 461.
16. V. Nekvasil, "The crystal field for Nd^{3+} in garnets," Phys. Status Solidi **87**(1), 317–323 (1978).
17. U. R. Rodríguez-Mendoza, S. F. León-Luis, J. E. Muñoz-Santiuste, D. Jaque, and V. Lavín, "Nd^{3+}-doped $Ca_3Ga_2Ge_3O_{12}$ garnet: A new optical pressure sensor," J. Appl. Phys. **113**(21), 213517 (2013).
18. A. Kaminska, R. Buczko, W. Paszkowicz, H. Przybylinska, E. Werner-Malento, A. Suchocki, M. Brik, A. Durygin, V. Drozd, and S. Saxena, "Merging of the $^4F_{3/2}$ level states of Nd^{3+} ions in the photoluminescence spectra of gadolinium-gallium garnets under high pressure," Phys. Rev. B **84**(7), 075483 (2011).
19. T. H. Allik, S. A. Stewart, D. K. Sardar, G. J. Quarles, R. C. Powell, C. A. Morrison, G. A. Turner, M. R. Kokta, W. W. Hovis, and A. A. Pinto, "Preparation, structure, and spectroscopic properties of Nd^{3+}:$\{La_{1-x}Lu_x\}_3[Lu_{1-y}Ga_y]_2Ga_3O_{12}$ crystals," Phys. Rev. B **37**(16), 9129–9139 (1988).
20. K. Wu, B. Yao, H. Zhang, H. Yu, Z. Wang, J. Wang, and M. Jiang, "Growth and properties of Nd:$Lu_3Ga_5O_{12}$ laser crystal by floating-zone method," J. Cryst. Growth **312**(24), 3631–3636 (2010).
21. Z. Jia, A. Arcangeli, J. Zhang, and C. Dong, "Efficient $Nd^{3+}\rightarrow Yb^{3+}$ energy transfer in Nd^{3+},Yb^{3+}:$Gd_3Ga_5O_{12}$ multicenter garnet crystal," J. Appl. Phys. **105**, 083113 (2009).
22. O. Guillot-Noël, B. Bellamy, B. Viana, and D. Gourier, "Correlation between rare-earth oscillator strengths and rare-earth–valence-band interactions in neodymium-doped Y*M*O_4(*M*=V, P, As), $Y_3Al_5O_{12}$, and $LiYF_4$ matrices," Phys. Rev. B **60**(3), 1668–1677 (1999).
23. A. A. Deminovich, A. P. Shkadarevich, and M. B. Dansilov, "Comparison of cw laser performance of Nd:KGW, Nd:YAG, Nd:BEL, and Nd:YVO_4 under laser diode pumping," Appl. Phys. B **67**(1), 11–15 (1998).
24. M. Inokuti and F. Hirayama, "Influence of energy transfer by the exchange mechanism on donor luminescence," J. Chem. Phys. **43**(6), 1978 (1965).
25. V. Lupei and A. Lupei, "Emission dynamics of the $^4F_{3/2}$ level of Nd^{3+} in YAG at low pump intensities," Phys. Rev. B **61**(12), 8087–8098 (2000).
26. K. Maeda, N. Wada, M. Umino, M. Abe, Y. Takada, N. Nakano, and H. Kuroda, "Concentration dependence of fluorescence lifetime of Nd^{3+}-doped $Gd_3Ga_5O_{12}$ lasers," Jpn. J. Appl. Phys. **23**(10), L759–L760 (1984).
27. J. E. Geusic, H. M. Marcos, and L. G. Van Uitert, "Laser oscillations in Nd-doped yttrium aluminum, yttrium gallium and gadolinium garnets," Appl. Phys. Lett. **4**(10), 182 (1964).
28. J. Löhring, K. Nicklausa, N. Kujatha, and D. Hoffmann, "Diode pumped Nd : YGG laser for direct generation of pulsed 935 nm radiation for water vapour measurements," Proc. SPIE **6451**, 64510I (2007).
29. C. Maunier, J. L. Doualan, R. Moncorge, A. Speghini, M. Bettinelli, and E. Cavalli, "Growth, spectroscopic characterization, and laser performance of Nd:$LuVO_4$, a new infrared laser material that is suitable for diode pumping," J. Opt. Soc. Am. B **19**(8), 1794–1800 (2002).

1. Introduction

Since the discovery of the laser, the use of the trivalent Neodymium (Nd^{3+}) ion-doped inorganic materials have attracted great attention in many areas, from science research to industry applications. Nd^{3+} ions exhibit broad and strong absorption band around 800 nm and a very intense emission around 1.06 μm, following a "four-level" scheme. Further, the $^4F_{3/2}$ emitting state can be conveniently populated by low-cost, commercially available laser diodes [1]. In addition, it has many intense pumping levels and efficient up-converted emissions [2].

Among different host materials, garnet crystals have always been attractive gain media for laser applications due to their high mechanical strength and good thermal and optical properties, such as high density, high thermal conductivity, good chemical stability, highly isotropic, high transparency from UV to mid IR region, and relatively low-energy phonons,

#240253 Received 5 May 2015; revised 23 Jun 2015; accepted 23 Jun 2015; published 2 Jul 2015

making them one of the most important families of host matrices for the trivalent rare earth (RE^{3+}) ions. Nd^{3+}-doped $Y_3Al_5O_{12}$ (YAG) garnet has been traditionally considered as the standard laser material, even though it shows a low effective distribution coefficient of Nd^{3+} ions and lack of ideal garnet structure for higher radii RE^{3+} ions, limiting the doping concentration to only a few atomic percent [3]. These disadvantages can be overcome by replacing aluminum atoms with gallium ones, since these garnets have larger unit cell volumes, higher refractive index and higher RE^{3+} solubility, thus showing larger oscillator strengths and stimulated emission cross-sections, lower pump threshold and higher laser efficiencies [3,4]. In the last decade, much efforts have been spent in the study of the luminescence properties of RE^{3+}-doped $Gd_3Ga_5O_{12}$ (GGG), $Y_3Ga_5O_{12}$ (YGG) and $Lu_3Ga_5O_{12}$ (LuGG) nanocrystalline garnets [5–8], especially in the development of lasers and phosphors in lightning, 3-D optical imaging for displays, bio-imaging, and as an alternative to quantum dots in photonic devices.

The ability to predict and control the luminescence properties of RE^{3+}-doped systems concerns the interactions occurring in its first coordination shell, where factors such as bond lengths and angles, coordination number, and covalency determine the energy, mixing, and splitting of the electronic states involved in the absorption and luminescence spectra [9]. The customary approach for investigating the relationship between local environment and optical properties is through variations of the chemical composition, in order to systematically vary the lanthanide-ligands bond distances and angles and gain useful information in developing a predictive capability. This size effect can be illustrated by the concept of internal pressure exerted by the host on the dopant, an approach known as chemical pressure.

In this work, we study of the effects of chemical pressure on the structure, and hence, on the vibrational and optical properties of the Nd^{3+} ion in a series of $RE_3Ga_5O_{12}$ gallium nano-garnets when the size of the RE^{3+} (= Gd^{3+}, Y^{3+}, Lu^{3+}) changes. The chemical pressure will modulate the structural, vibrational and elastic properties of the nano-garnet. In addition, the crystal-field interaction felt by the RE^{3+} ions is expected to be different in these three host lattices due to the magnitude of the size mismatch with the ligands [10]. The size effects also generate stresses, strains and rearrangements in the first coordination sphere of the Nd^{3+} optically active ion, entering as dopant in the nano-garnets, which modifies not only the local structure but also the expansion of the *4f* wave functions due to the increased covalent bonding. Further modifications of free-interactions and of crystal-field, and hence, in the optical properties are then induced.

As far as we know, there are no works on $Gd_3Ga_5O_{12}$, $Y_3Ga_5O_{12}$ and $Lu_3Ga_5O_{12}$ gallium nano-garnets doped with Nd^{3+} ions synthesized by a low-cost, low-temperature and environmental friendly sol-gel technique. The exact knowledge of the structural properties and their correlation with vibrational and optical properties is of paramount importance for photonics applications, the real target to be achieved with these nanomaterials.

2. Experimental

Nano-garnets of composition $RE_{3(1-x)}Nd_{3x}Ga_5O_{12}$ (where RE = Gd, Y, and Lu, and x = 0.01; labeled as GGG1Nd, YGG1Nd, and LuGG1Nd, respectively) were synthesized by citrate sol-gel method [5–7]. X-ray diffraction (XRD) patterns were measured on a diffractometer (PANalytical X'Pert Pro) using $CuK\alpha_1$ radiation. Infrared absorption and Raman spectra were recorded using a spectrometer (FTIR Bruker IFS66) and a microspectrometer (Horiba Jobin-Yvon LabRAM HR UV, equipped with a HeNe laser), respectively. A spectrophotometer (Cary 5000) was used to measure the diffuse reflectance spectra. The luminescence spectra were measured by exciting with cw tunable Ti:sapphire laser (Spectra Physics 3900S) pumped by a 10 W cw Ar^+ laser (Spectra Physics 2060-10 Beamlock). The emission was focused onto a 0.32 m monochromator (Jobin Yvon Triax 320) coupled with thermoelectric photomultipliers (Hamamatsu R5108 and H10330B-75). The luminescence decay curves were obtained exciting with a 10 ns pulsed optical parametric oscillator

#240253 Received 5 May 2015; revised 23 Jun 2015; accepted 23 Jun 2015; published 2 Jul 2015

(EKSPLA/NT342/3/UVE) using a digital storage oscilloscope (LeCroy WS424) coupled to the detection system. Spectra were corrected from the instrument responses and made at room temperature.

3. Results and discussion

3.1. Structural properties

X-ray powder diffraction patterns for GGG1Nd, YGG1Nd, and LuGG1Nd nano-garnets are shown in Fig. 1. All the reflections in the profiles of the powder samples are well indexed to a single cubic (bcc) phase with space group *Ia*-3*d* (No. 230, Z = 8), where no impurity phase has been detected. Crystal structure parameters have been obtained after fitting the profiles of the nano-garnets by the Rietveld method using the FULLPROF program [11]. As can be seen from Table 1, quite goodness of fitting parameters (see the reliability factors - χ^2, R_p, R_{wp}, and R_{exp}) has been noticed and only small differences have been found for the amplitudes of few peaks (see Fig. 1). Two main features can be outlined from these results: i) the crystalline structures of the gallium nano-garnets are very similar to those of their bulk counterparts (for example, the experimental unit cell parameter for the bulk LuGG, 12.19 Å [12], is practically equal to that of the LuGG nanoparticles, 12.2 Å) and, ii) the decrease in the values of the cell parameter *a* (see Table 1) and, hence, in the volume *V* of the unit cell (see Fig. 2 and Table 2) when Gd^{3+} ions are replaced by Y^{3+} and Lu^{3+} ones, which can be related to the difference in their ionic radii, $r(Gd^{3+}) = 1.05$ Å > $r(Y^{3+}) = 1.02$ Å > $r(Lu^{3+}) = 0.98$ Å.

Table 1. Cell parameters and reliability factors obtained from the Rietveld refinement.

Compound	*a* (Å)	χ^2	R_p	R_{wp}	R_{exp}
$Gd_3Ga_5O_{12}$:Nd	12.4241(2)	2.44	16.1	12.3	5.94
$Y_3Ga_5O_{12}$:Nd	12.3055(2)	2.15	13.4	14.2	2.83
$Lu_3Ga_5O_{12}$:Nd	12.1893(3)	2.01	16.9	18.2	2.71

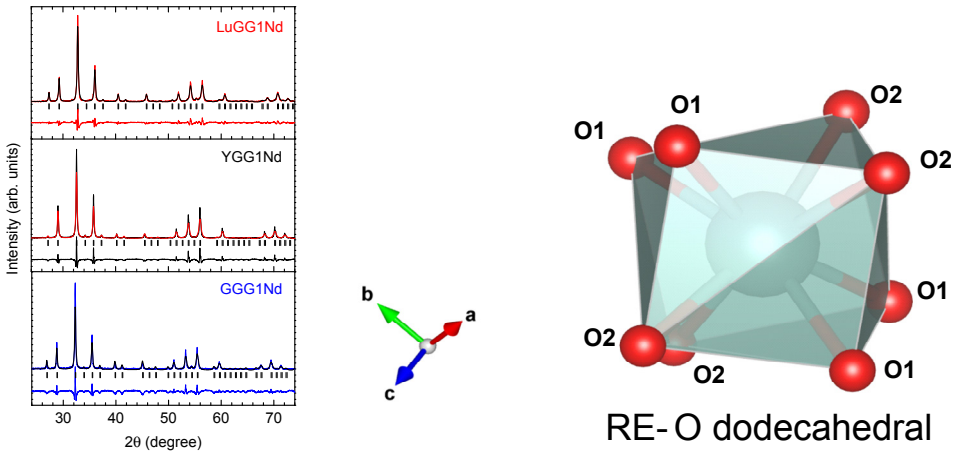

Fig. 1. (Left) X-ray diffraction patterns of $Gd_3Ga_5O_{12}$ (GGG1Nd), $Y_3Ga_5O_{12}$ (YGG1Nd), and $Lu_3Ga_5O_{12}$ (LuGG1Nd) gallium nano-garnets doped with 1 mol% of Nd^{3+} ions. Rietveld refinements including difference between calculated and observed patterns are also shown. (Right) Picture of the RE-O dodecahedral unit.

When the size of the nanoparticles is very small (< 5 nm) it is quite typical to observe distortions of the crystalline structure due to the high surface-to-volume ratio, which further affect the vibrational and optical properties of the material, but that may disappear when the size of the nanoparticles increases [13]. The average crystallite size *D* of the nano-garnets has been calculated by using the Scherrer's formula ($D = 0.89\lambda/\beta\cos\theta$, where $\lambda = 1.5406$ Å is the

#240253 Received 5 May 2015; revised 23 Jun 2015; accepted 23 Jun 2015; published 2 Jul 2015

incident wavelength of X-rays, β is the full width at half maximum of the peaks, and θ is the angle of diffraction), giving estimations of around 40, 45 and 45 nm for GGG1Nd, YGG1Nd and LuGG1Nd nano-garnets, respectively. The most intense peaks at 2θ angles, i.e., at 32.38309 for GGG1Nd, at 32.74405 for YGG1Nd, and at 32.94458 for LuGG1Nd have been used for these calculations. In order to obtain nanoparticles in the form of pure garnet structure, the sol-gel synthesis needs thermal treatments that give rise to particles of sizes not smaller than 40 nm. We can still talk about *nano* (particle size<100 nm), but in fact what we observe in these nanoparticles is that we can achieve the same properties as the garnet bulk materials but with smaller particle size. As a conclusion, our results show that these nanoparticles have essentially bulk garnet structural properties and, as it will be shown later in this paper, the same applies for the vibrational and optical properties, which may open new and interesting optical and photonic applications with increased resolution with respect to conventional bulk phosphors.

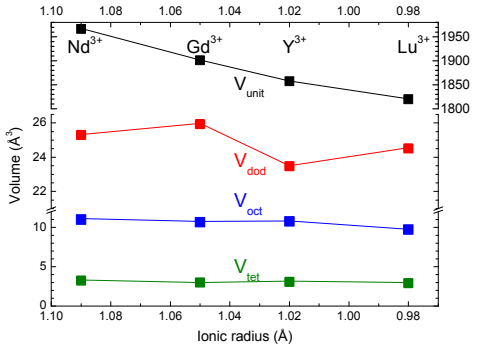

Fig. 2. Volumes of unit cell (black), RE^{3+}-O dodecahedron (red), Ga-O octahedron (blue) and Ga-O tetrahedron (green) of the nanocrystalline gallium garnet as a function of the ionic radius of the RE^{3+} ions. Data for $Nd_3Ga_5O_{12}$ nano-garnet have been also included for comparison.

Table 2. Bond distances of the RE and Ga ions.

Compounds	RE-O1* RE-O2* (Å)	Ga_{oct}-O (Å)	Ga_{tet}-O (Å)
$Nd_3Ga_5O_{12}$	2.417 2.501	2.025	1.861
$Gd_3Ga_5O_{12}$	2.458 2.512	2.000	1.786
$Y_3Ga_5O_{12}$	2.368 2.431	2.014	1.828
$Lu_3Ga_5O_{12}$	2.403 2.471	1.941	1.786

* RE = Nd, Gd, Y or Lu

The $RE_3Ga_5O_{12}$ garnet crystalline structures can be described as a three dimensional network of GaO_4 tetrahedra (S_4 point symmetry) and GaO_6 octahedra (S_6 point symmetry) linked by sharing oxygen ions at the corners of the polyhedra [6]. These polyhedra are arranged in chains along the three crystallographic directions and form dodecahedral cavities that are occupied by the RE^{3+} (Nd, Gd, Y, or Lu) ions with a D_2 point symmetry. The difference in the ionic radii of these RE^{3+} ions is associated to the rare earth, or lanthanide, contraction effect, and it has its origin in the fact that the filling of the *4f* orbital through the lanthanide series poorly screens the increasing nuclear charge. Thus the increasing effective nuclear charge strongly attracts the outer electrons and gives rise to a decrease in the

#240253 Received 5 May 2015; revised 23 Jun 2015; accepted 23 Jun 2015; published 2 Jul 2015

dimensions of the RE electron shells over the series. A special mention must be paid to Y^{3+} ion, which is a transition metal ion but it is often classified as a rare earth ion due to their chemical similarities. The differences in the ionic radii of Gd^{3+}, Y^{3+} and Lu^{3+} ions have a dramatic effect on the cubic structure of the garnet structure by reducing the volume of the unit cell by a 5% (see Fig. 2), an effect clearly observed in the shift of diffraction peaks to higher Bragg's angles when passing from Gd^{3+} to Lu^{3+}, taking into account the Bragg's equation, where the angle is inversely proportional to the inter-planar distance that is proportional to the unit cell size. This gives rise to successive more compacted arrangements of atoms, and hence with smaller RE-O distances, that result in a stronger crystal-field interaction between the oxygen ligands and the RE^{3+} ions.

The decrease of the unit cell volume is in clear correspondence with the decrease of the volumes of the GaO_4 tetrahedron (−12%) and the GaO_6 octahedron (−5%), as can be seen in Fig. 2, although with asymmetrical changes when compared to those results found for the YGG1Nd nano-garnet, necessary entailed in order to keep the right unit cell volume. Anyhow, this "size effect" produces a drastic descrease of around −15% of the dodecahedron cavity volume (see RE-O arrangement in Fig. 1), correlated with its higher compressibility compared to the Ga-O arrangements.

Except for the special Y^{3+} ions, which shows a noticeable decrease of the RE-O bond distances (see Table 2), the distance from the RE^{3+} ions to the oxygen ligands in the dodecahedral site decreases when the ionic radius of the central ion decreases, i.e. when replacing Gd^{3+} for Lu^{3+}, giving rise to stronger crystal-field interactions between the RE^{3+} ions and their oxygen ligands. In addition, the two sets of distances, i.e. RE-O1 and RE-O2, are also closer in magnitude (see Table 2), making the faces of the dodecahedral site more planar (see Fig. 1) and, hence, reducing the orthorhombic distortion. In this scenario, and due to ionic size considerations in the $RE_3Ga_5O_{12}$ lattices, the doping Nd^{3+} ions [$r(Nd^{3+})$ = 1.109 Å] are expected to enter predominantly into the distorted dodecahedral sites by replacing the Gd^{3+}, Y^{3+} or Lu^{3+} ions. However, the degree of disorder or distortion of the Nd^{3+} sites, which is expected to increase with the decrease of the dodecahedral volume due to the size mismatch, cannot be clearly stated through diffraction measurements.

3.2. Vibrational characterization

In order to understand the effects of the chemical pressure on vibrational frequencies in the gallium nano-garnets, especially those which play a key role in the Nd^{3+} non-radiative multiphonon de-excitation processes, the infrared- and Raman-active modes have been measured (see Fig. 3). According to group theoretical considerations, the *Ia-3d* structure of $RE_3Ga_5O_{12}$ garnet has 98 vibrational modes that can be classified at the Brillouin Zone center as 25 Raman-active modes (Γ_R), 17 infrared-active modes (Γ_{IR}), 55 optically-inactive (silent) modes (Γ_S), and 1 acoustic (T_{1u}) mode [12].

The IR absorption spectra (see Fig. 3.left) of the three nano-garnets consist of two very broad bands with maxima at around 600 and 840 cm^{-1}. Depending on the RE^{3+} ion, these two bands show hyperfine structures of 4 or 5 peaks that are shifted in energy and with different intensities due to overlapping effects, making the identification of the 17 IR-active modes a difficult task. On the other hand, out of 25 predicted Raman-active modes, 17 of them are experimentally observed for the gallium nano-garnets (see Fig. 3.right). Assignments of the modes have been carried out on the basis of previous experiments and theoretical calculations [12] and, as it has been already mentioned, quite good agreements have been found between the vibrational modes of the $RE_3Ga_5O_{12}$ nanoparticles and their bulk single-crystal counterparts. In addition, the introduction of 1.0 mol% of Nd^{3+} ions does not affect the lattice dynamics of the garnet structures [12].

The complex IR and Raman spectra of nano-garnets can be interpreted on the basis of the vibrational modes of the GaO_4 tetrahedral, GaO_6 octahedral and REO_8 dodecahedral units. This approximation makes the discussion easier, although it has to be clearly stated that the

#240253 Received 5 May 2015; revised 23 Jun 2015; accepted 23 Jun 2015; published 2 Jul 2015

attribution of each mode to a single unit is not straightforward, since the vibrations of the different polyhedra are strongly coupled to each other. In this respect, the vibrational spectra of the $RE_3Ga_5O_{12}$ garnets can be divided into two main ranges: the low-frequency range (100–300 cm^{-1}), with a considerable contribution of vibrational modes of RE^{3+} ions, and the high-frequency range (300–800 cm^{-1}), with almost no contribution of RE^{3+} ions. We must note that both ranges are dominated by the vibrations of the GaO_4 and GaO_6 units.

The main feature of the vibrational spectra is that all the IR and Raman phonon frequencies exhibit a monotonous increase as the chemical pressure increases due to the decrease of the interatomic distances in the unit cell volume when replacing the Gd^{3+} ion for Y^{3+} and Lu^{3+} ones, in a similar way as when high pressure is applied on a garnet to reduce its volume using a diamond anvil cell [12].

Raman spectrum of the three garnets are represented in Fig. 3 (right). As it is clearly observed, the modes with the largest chemical pressure variations are those with frequencies above 300 cm^{-1}, which are related to vibrations of GaO_4 tetrahedra and GaO_6 octahedra. It is worth noting that the highest frequencies of the vibrations corresponding to tetrahedral and octahedra are found in the LuGG structure. This can be explained taking account the variations of local internal parameters of the polyhedra that constitute the garnet unit cell. The bond distances of the polyhedra are shown in Table 2 and it is observed that the smaller the ionic radius of RE^{3+} is, the smaller the unit cell volume is and the smaller the Ga-O distances in the tetrahedra and octahedra are. Therefore, the restoring forces between the Ga and O atoms increase and the phonon frequencies of the tetrahedra and octahedra increase with the increase of the chemical pressure.

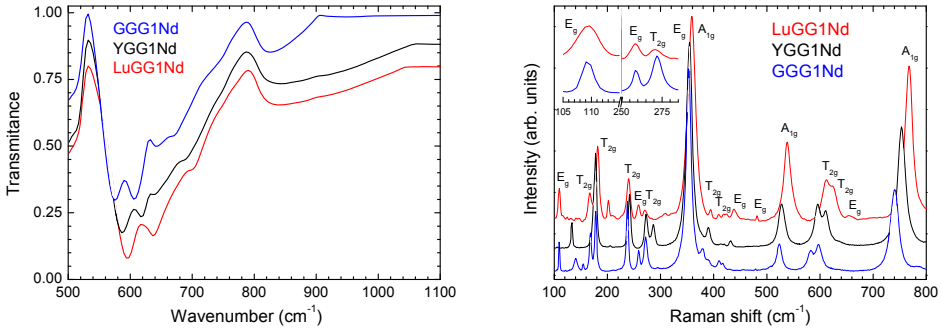

Fig. 3. (Left) Infrared absorption and (right) Raman spectra of the gallium nano-garnets. The spectra of the $Y_3Ga_5O_{12}$ and $Lu_3Ga_5O_{12}$ nano-garnets have been shifted in transmission and intensity a fixed amount for comparison purpose.

The low-frequency region, only measured for the Raman-active modes, is dominated by translational movements of the GaO_4 tetrahedron and REO_8 dodecahedron. The phonon frequencies of GaO_4 increase as the size of the RE decreases, as occurs in the high-frequency range. On the contrary, the two lowest-energy E_g and T_{2g} phonons at 110 and 167 cm^{-1}, respectively, and the E_g mode (258 cm^{-1}) and the T_{2g} mode (271 cm^{-1}) in the GGG garnet decrease in frequency when the chemical pressure increases from Gadolinium to Lutetium. This is due to the fact that these modes are associated to the vibrations of the dodecahedra. Therefore, they exhibit a clear dependence on the mass of the RE atom since the frequencies are expected to decrease for heavier RE atoms in the garnet structure. This dependence also explains the large differences of the YO_8 vibrational modes with respect to those corresponding to other RE_8, since they can be directly correlated with the much smaller mass of the Y atoms than of RE atoms. Curiously, the modes in the YGG nanogarnet above 300 cm^{-1} have frequencies which are intermediate between those of GGG and LuGG nanogarnets,

#240253 Received 5 May 2015; revised 23 Jun 2015; accepted 23 Jun 2015; published 2 Jul 2015

despite the Ga-O distances in the YGG nanogarnet are larger than those of GGG nanogarnet and, therefore, should exhibit smaller frequencies. This result can be understood by the coupling of all polyhedra in the different vibrations and the compensation effects of the larger Ga-O distances (leading to smaller frequencies) and the smaller mass of Y atom (leading to larger frequencies of all the modes of the compound) compared to those values in the GGG nanogarnet.

3.3. Optical properties

Optical spectroscopy is a powerful technique that can throw light on the influence of the chemical pressure on the optical properties of the Nd^{3+} ion and its correlation with its real immediate environment in the gallium nano-garnets under study. The optical properties of the Nd^{3+} ions and, therefore, their interest for optical and photonic applications depend on the local structure of these ions in the nano-garnets, since it rules the fine structure splitting of the free-ion multiplets and the forced intra-configurational *4f-4f* electric-dipole transition probabilities in the optical (UV-Vis-NIR) range [14]. In the gallium nano-garnets under study, the Nd^{3+} ions will predominantly enter the distorted dodecahedral sites by replacing the RE^{3+} (Gd, Y, or Lu) ions without charge compensation. Thus the eight oxygen ligands surrounding the optically active Nd^{3+} ion create a local environment with orthorhombic D_2 point symmetry. As a consequence, the D_2 crystal-field interaction felt by the optically active ion will completely remove the degeneracy of the $^{2S+1}L_J$ multiplets of the free-Nd^{3+} ion (except for the Kramers degeneracy) giving rise to (2J + 1)/2 Stark, or crystal-field, levels labelled according to the D_2 irreducible representations. The changes in the bond distances and angles between the Nd^{3+} and their ligands due to chemical pressure will also modify the crystal-field interaction, which will be reflected as changes in the energy level diagram and the absorption and emission spectra of the Nd^{3+} ions in the different nano-garnets.

The first step in this study is the measurement of the diffuse reflectance spectra of the $RE_3Ga_5O_{12}$ nano-garnets doped with 1.0 mol% of Nd^{3+} in the visible-NIR range, which are given in Fig. 4. The peaks observed correspond to intra-configurational $4f^3$-$4f^3$ electronic transitions starting from the $^4I_{9/2}$ ground state to the different excited levels of the Nd^{3+} ion, assumed to be electric-dipole in nature. The sharp peak profiles found for all the electronic transitions confirms that the Nd^{3+} ions are incorporated in the nanocrystalline structure of the garnet. The labels of the different transitions of the Nd^{3+} ion in the gallium nano-garnets have been assigned according to the well-known Dieke's diagram for this ion and the energies of the Stark levels of Nd^{3+} in $RE_3Ga_5O_2$ single crystals summarized by Morrison and Leavitt [15] and Nekvasil [16]. The main fact is that the relative intensities (directly proportional to the absorption probabilities) and the fine-structure of the bands are closely similar for the three nano-garnets, but with slight and measurable differences in the energies of the fine structure of peaks of each band. These differences can be clearly observed for the $^4I_{9/2} \rightarrow {}^2H_{9/2}, {}^4F_{5/2}$ transitions given in Fig. 4 (right). When analyzing this absorption transition for the GGG1Nd, YGG1Nd and LuGG1Nd nano-garnets, and as a general feature, there is a combination of a slight red-shift and a reduction of the energy gaps between peaks, and hence in the splitting of the multiplets, with the decrease of the dodecahedron volume.

#240253 Received 5 May 2015; revised 23 Jun 2015; accepted 23 Jun 2015; published 2 Jul 2015

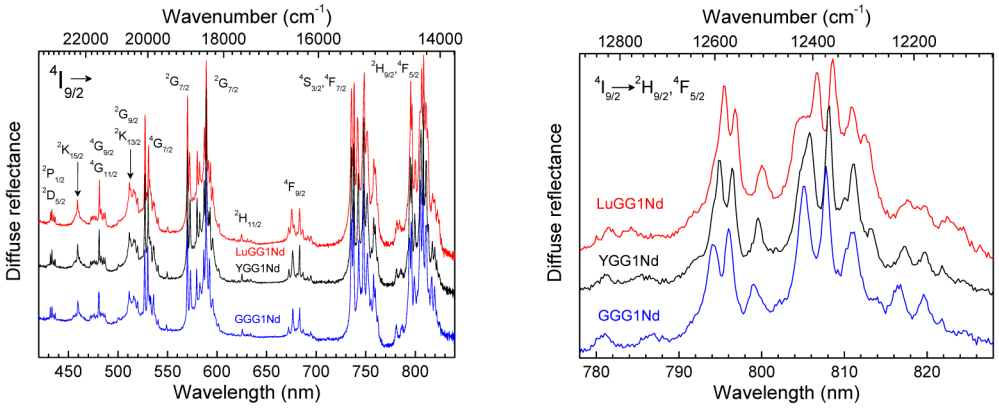

Fig. 4. (Left) Diffuse reflectance spectra of the gallium nano-garnets. (Right) The $^4I_{9/2}\rightarrow{}^2H_{9/2},{}^4F_{5/2}$ transitions are compared for the three gallium nano-garnets. The spectra of the $Y_3Ga_5O_{12}$ and $Lu_3Ga_5O_{12}$ nano-garnets have been shifted in intensity a fixed amount for comparison purpose.

These effects are also observed, in a larger scale, in the luminescence spectra of 1.0 mol% of Nd^{3+} ions in the three gallium nano-garnets under cw 805 nm laser excitation, in resonance with the $^4I_{9/2}\rightarrow{}^2H_{9/2},{}^4F_{5/2}$ transitions (see Fig. 5), that immediately populates, via multiphonon de-excitation of the Nd^{3+} ions, the two thermalized emitting levels of the $^4F_{3/2}$ multiplet. Three main NIR bands are normally observed, associated to the $^4F_{3/2}\rightarrow{}^4I_{9/2}$ transition in the 860-960 nm range, to the $^4F_{3/2}\rightarrow{}^4I_{11/2}$ transition in the 1050-1130 nm range and to the $^4F_{3/2}\rightarrow{}^4I_{13/2}$ transition in the 1310-1430 nm range. At this point it is worth noting that the relative intensities of each spectrum have been corrected from the instrument response and normalized to the maximum intensity of the $^4F_{3/2}\rightarrow{}^4I_{11/2}$ transition, and that they can be compared taking into account that the spectra of the YGG1Nd and LuGG1Nd nano-garnets have been vertically shifted by a fixed constant value. Again, the peaks associated to transitions from the thermalized Stark levels to the low energy Stark levels of the ^4I_J multiplets clearly show a decrease in the splitting of these multiplets.

From the absorption and emission spectra, a partial energy level diagrams of the Nd^{3+} ion in the $RE_3Ga_5O_{12}$ nano-garnets are given in Fig. 6 (left), showing interesting differences that can be directly associated to the increase of the crystal-field strength felt by the Nd^{3+} ions when reducing the size of the RE^{3+} ion (Gd^{3+}, Y^{3+} or Lu^{3+}) in the dodecahedral sites of the gallium nano-garnets [10]. When analysing the crystal-field interaction it is worth noting that the local symmetry at the Nd^{3+} sites in garnets is often described as an orthorhombic distortion of a main cubic symmetry [17]. Thus two contributions must be taken into account when describing the crystal-field interaction: the cubic symmetry component and, superimposed, the non-cubic symmetry component that accounts for the real D_2 symmetry at the Nd^{3+} sites. Using this description, the cubic symmetry splits the ground $^4I_{9/2}$ multiplet in three levels ($\Gamma_6 + 2\Gamma_8$) while keeping the lowest emitting $^4F_{3/2}$ level as a Γ_8 singlet (see Fig. 6.right). For the $^4I_{9/2}$ ground multiplet, the non-cubic distortion removes the remaining degeneracy and each Γ_8 cubic-level splits in two Stark doublets (Z_1-Z_4 Stark levels), leaving the Γ_6 singlet (Z_5 Stark level) well separated (around 500 cm^{-1}) from the rest. Interestingly, for the $^4F_{3/2}$ multiplet it can be concluded that the non-cubic part of the crystal-field interaction must be directly responsible for the observed splitting into the R_1 and R_2 Stark emitting levels, which can be taken as a rough measurement of the magnitude of the non-cubic orthorhombic distortion from the main cubic field [17].

#240253 Received 5 May 2015; revised 23 Jun 2015; accepted 23 Jun 2015; published 2 Jul 2015

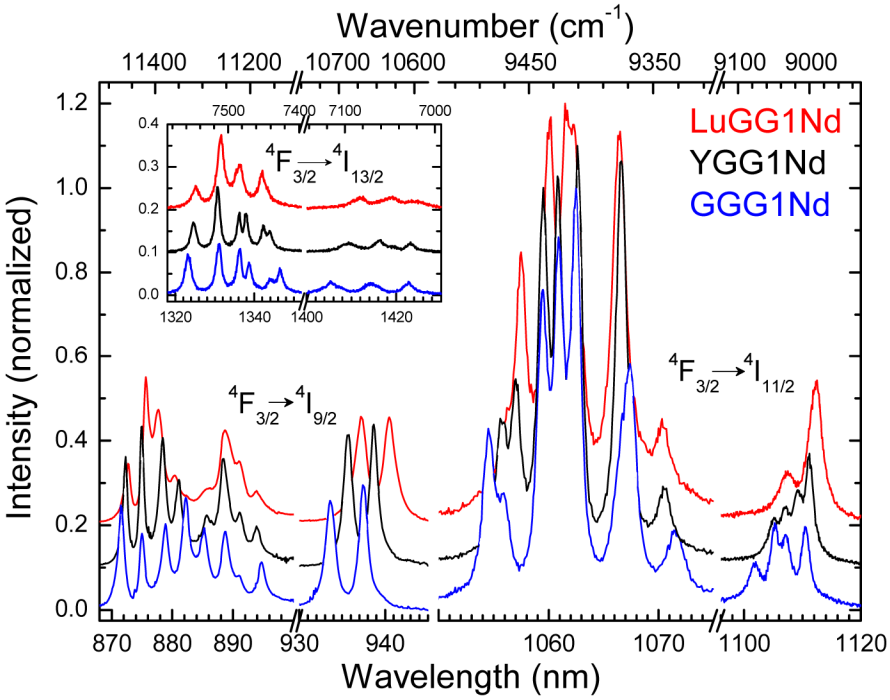

Fig. 5. Emission spectra of the three gallium nano-garnets after exciting resonantly the $^4I_{9/2}\rightarrow{}^2H_{9/2},{}^4F_{5/2}$ transitions with a laser light at 805 nm. Intensities are normalized to the maximum of the $^4I_{9/2}\rightarrow{}^2H_{9/2},{}^4F_{5/2}$ transition and shifted a fixed amount for the $Y_3Ga_5O_{12}$ and $Lu_3Ga_5O_{12}$ nano-garnets for comparison purpose. The relative intensities of all the emissions can be directly compared.

The contraction of the peaks of the $^4F_{3/2}\rightarrow{}^4I_J$ transitions as well as the red-shift of the low-energy peaks in the luminescence spectra when the volume of the dodecahedron decreases by reducing the ionic radius of the RE^{3+} ions, i.e. when the chemical pressure over the dodecahedral sites increases, can be understood taking into account various factors. Starting with the $^4F_{3/2}$ multiplet, the R_1-R_2 energy gap is lower in LuGG (~37 cm^{-1}) and YGG (~35 cm^{-1}) than for GGG (~44 cm^{-1}) gallium nano-garnets, while its barycenter, or centroid, also decreases in energy. At the same time, the Z_1-Z_4 Stark levels of the $^4I_{9/2}$ multiplet scarcely decrease in energy and become closer in energy, being the Z_5 the only one that increases. The combination of these factors is due to the stronger crystal-field strength felt by the Nd^{3+} ions, as well as a higher degree of covalency of the Nd^{3+}-ligands bonds in LuGG1Nd than in YGG1Nd and GGG1Nd gallium nano-garnets. The former increases the hyperfine splitting of the $^{2S+1}L_J$ multiplets, whereas the latter produces an overall contraction of the $4f^3$ ground configuration. Similar results have been found in different crystalline garnets when high pressure techniques are applied [17].

Special attention has to be paid to the splitting of the $^4F_{3/2}$ multiplet, since the R_1-R_2 energy gap decreases as the chemical pressure increases; an effect also observed in the Γ_8 levels of the $^4I_{9/2}$ ground multiplet. If there is a smaller dodecahedron volume, leading to smaller RE-O distances, an increase of the splitting of the multiplet is expected. In addition, the large ionic radius of the Nd^{3+} ion is also expected to increase the distortion of the dodecahedron, especially in the case of YGG and LuGG in which the size mismatch of the Nd^{3+} and the RE^{3+} ions are larger. However, in the case of the nano-garnets, as the chemical pressure increases the redistribution of the bond distances (RE-O1 and RE-O2 are increasingly closer in value) and angles of the dodecahedron effectively decrease the orthorhombic distortion. In other words, the local symmetry of the Nd^{3+} site in the garnet

#240253 Received 5 May 2015; revised 23 Jun 2015; accepted 23 Jun 2015; published 2 Jul 2015

structure moves closer to cubic when the chemical pressure increases, leading to a smaller splitting of the Γ_8 levels. An effect also observed in high pressure experiment in Nd^{3+}-doped garnet crystals [17]. However, it is worth noting that the dodecahedral unit will never reach the cubic structure, even when the Nd-O1 and Nd-O2 distances may become equal applying high pressure with a diamond anvil cell [18].

On the other hand, it is well known that the branching ratio is a critical parameter for laser design as it characterizes the stimulated emission from any specific transition. Hence, branching ratios have been evaluated for the $^4F_{3/2}\rightarrow{}^4I_J$ (J = 9/2, 11/2 and 13/2) main transitions of Nd^{3+} ion in the three gallium nano-garnets. The branching ratio of the $^4F_{3/2}\rightarrow{}^4I_{11/2}$ laser transition is found to be 0.71, 0.70 and 0.69 for LuGG1Nd, YGG1Nd, and GGG1Nd nano-garnets, respectively. These results are higher compared to those of Nd^{3+}-doped LaLuGG [19], LuGG [20] or GGG [21] single crystals. The intensity of the $^4F_{3/2}\rightarrow{}^4I_{11/2}$ transition could be increased due to (a) the increase of the odd part of the crystal-field interaction, which rules the intraconfigurational transitions; (b) the overlap of transitions between several closely spaced Stark levels of the ground and excited energy levels [22]; and/or (c) an intensity-borrowing mechanism through mixing of the 4f-5d orbitals of Nd^{3+} ion via the lattice valence band levels [23].

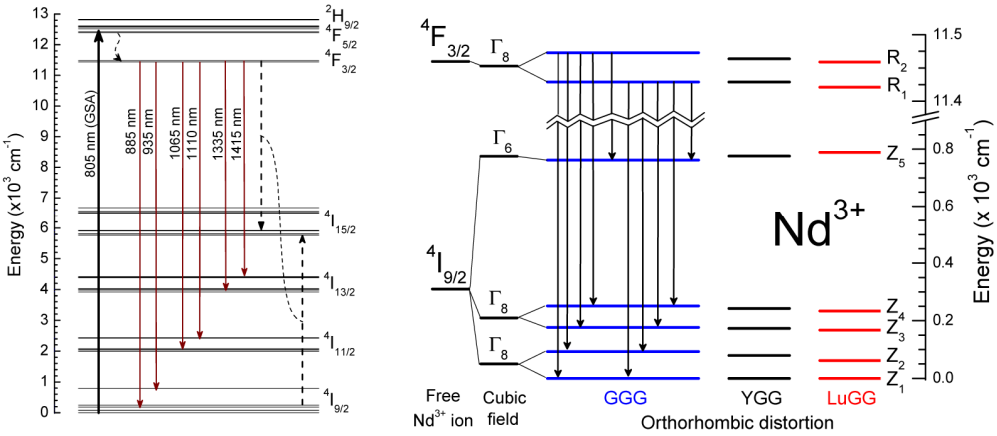

Fig. 6. (Left) Partial energy level diagram of the Nd^{3+} ion showing different radiative transitions (downward solid lines) related to the luminescence after a $^4I_{15/2}\rightarrow{}^2H_{9/2},{}^4F_{5/2}$ ground state absorption (GSA) under a direct laser excitation at 805 nm. The multiphonon (zig-zag lines) and energy transfer (dashed lines) non-radiative relaxation processes are also shown. (Right) Partial energy level diagram of the Nd^{3+} ion corresponding to the Stark levels of the $^4F_{3/2}$ and $^4I_{9/2}$ multiplets and the transitions between the Stark levels in the nano-garnets under study.

In addition to a high branching ratio for laser or amplification applications, it is also necessary to have longer lifetimes for the $^4F_{3/2}$ level of Nd^{3+} ions. The luminescent decay curves for the $^4F_{3/2}$ level of Nd^{3+} ions were measured by exciting with an 805 nm pulsed laser and monitoring the $^4F_{3/2}\rightarrow{}^4I_{9/2}$ emission at around 878 nm (see Fig. 7). The decay curves exhibit a slight non-exponential nature for short times. Single exponential dynamics are only expected at low concentration of Nd^{3+} ions, where interactions among the optically active ions are negligible. As the Nd^{3+} concentration increases, and due to the presence of multipolar interactions between them, the decay curves show non-exponential behavior associated with the quasi-resonant energy transfer cross-relaxation ($^4F_{3/2}$, $^4I_{9/2}$)$\rightarrow$($^4I_{15/2}$, $^4I_{15/2}$) channel (see dotted lines in Fig. 6.left). In addition, the presence of Nd^{3+}-Nd^{3+} pairs and a small fraction of Nd^{3+} ions in octahedral sites may also contribute to the non-exponential behavior of the luminescence decay curves [10].

#240253 Received 5 May 2015; revised 23 Jun 2015; accepted 23 Jun 2015; published 2 Jul 2015

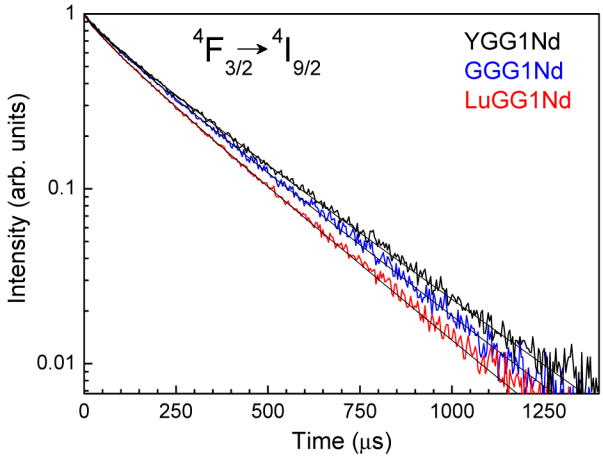

Fig. 7. Luminescence decay curves of the $^4F_{3/2}$ level monitoring the $^4F_{3/2} \rightarrow {}^4I_{9/2}$ transition at around 888 nm after exciting resonantly the $^4I_{9/2} \rightarrow {}^4G_{7/2}$ transition with a pulsed laser light at 532 nm. Fitted curves (in black) to the Inokuti-Hirayama model (with $S = 6$) are also given.

These multipolar interactions can be understood in the frame of the Inokuti–Hirayama model [24], which shows that the fluorescence decay intensity $I(t)$ after laser pulse excitation is given by

$$I(t) = I_0 \exp\left[-\left(\frac{t}{\tau_0}\right) - Q\left(\frac{t}{\tau_0}\right)^{3/S}\right] \quad (1)$$

where τ_0 is the intrinsic lifetime of the donor in the absence of acceptor; S = 6, 8 or 10 depending on whether the dominant mechanism of the interaction between Nd^{3+} ions is dipole–dipole, dipole-quadrupole or quadrupole-quadrupole, respectively; and the energy transfer parameter Q is defined as

$$Q = \frac{4\pi}{3}\ \Gamma\left(1-\frac{3}{S}\right)\ N_0\ R_0^3 \quad (2)$$

where N_0 is the concentration of acceptors (that it is almost equal to the total concentration of RE^{3+} ions that act as acceptor); and R_0 is the critical transfer distance defined as the donor-acceptor separation for which the rate of energy transfer to the acceptors is equal to the rate of intrinsic decay of the donor.

The decay curves of GGG1Nd, YGG1Nd and LuGG1Nd nano-garnets have been well fitted to Inokuti-Hirayama model (see Fig. 7) considering $S = 6$, confirming the existence of a major contribution of dipole-dipole interactions between the Nd^{3+} ions to the energy transfer processes in these gallium nano-garnets. The limitation of the multipolar ion–ion interaction that induces this transfer to dipole–dipole contribution is in agreement with the selection rules for the levels involved in the transition, which preclude the quadrupolar transitions. Similar results have been found in Nd^{3+} doped LaLuGG, YAG and GGG single crystals [19, 25, 26].

The intrinsic lifetime and energy transfer parameter are derived from the fitting process: the τ_0 values are found to be 290, 315, and 275 μs (with an uncertainty of ± 6 μs), and for the Q parameter the values are found to be 0.29, 0.34, and 0.36 (with an uncertainty of ± 0.03) for GGG1Nd, YGG1Nd and LuGG1Nd nano-garnets, respectively. These results show the competition between higher spontaneous emission and multiphonon relaxation rates ($1/\tau_0 = A + W_{MP}$) and the energy transfer probabilities when chemical pressure (RE size) increases (decreases), although it seems that it is slightly better for the YGG nano-garnet. However, and

#240253 Received 5 May 2015; revised 23 Jun 2015; accepted 23 Jun 2015; published 2 Jul 2015

taking into account the uncertainty of the transfer parameter, the energy transfer interactions among Nd^{3+} ions seem to be rather similar for the three nano-garnets, not showing the expected large increase when the RE-RE distances are reduced (Gd-Gd = 3.804 Å, Y-Y = 3.768 Å, and Lu-Lu = 3.732 Å) with the chemical pressure. In addition, the τ_0 values for the $^4F_{3/2}$ level of Nd^{3+} ion in these gallium nano-garnets are found to be longer compared to those of Nd^{3+}-doped YAG, YGG, GGG, $LuVO_4$ and YVO_4 single crystals [23, 27–29]. This is a very interesting result because the longer luminescence lifetime for the $^4F_{3/2}$ level of Nd^{3+} ions in the present nano-garnets can reduce the pump threshold to get laser output at 1.06 μm emission of the $^4F_{3/2} \rightarrow {}^4I_{11/2}$ transition.

4. Conclusions

A correlation between the structures of rare earth gallium nano-garnets and the vibrational and optical properties of the Nd^{3+} ions incorporated as dopant has been derived. Chemical pressure can be achieved in gallium garnet structures by the simple substitution of the RE^{3+} (= Gd, Y, and Lu) ions due to their differences in ionic size (related to the rare earth contraction). The GaO_4, GaO_6 and REO_8 structural units reduce their volumes creating a more compacted unit cell when the RE size decreases. This size effect also increases the frequencies of the vibrational modes of the GaO_4 tetrahedra and the GaO_6 of the octahedra, whereas those associated with the REO_8 decreases due to the increase of the RE mass. Chemical pressure increases the crystal-field strength felt by the Nd^{3+} ions in the nano-garnet structure but, at the same time, the degree of orthorhombic distortion of the REO_8 dodecahedral unit decreases, giving rise to an overall smaller splitting of the $^4F_{3/2}$ emitting multiplet and, hence of the emission peaks to the lower Stark levels of each ^4I_J multiplet. The lifetime for the $^4F_{3/2}$ level of Nd^{3+} ion in these nano-garnets are quite close to each other, although they are found to be longer compared to those of other Nd^{3+}-doped crystals; whereas the energy transfer processes are mainly due to dipole-dipole type interaction between the Nd^{3+} ions and are nearly insensitive to the chemical pressure, i.e. when the RE-RE distance decreases. The competition between the Nd^{3+} radiative versus non-radiative de-excitation rates gives rise to strong luminescence at around 1.065 μm evidenced from high branching ratios of the $^4F_{3/2} \rightarrow {}^4I_{11/2}$ transition and relatively long lifetimes of the $^4F_{3/2}$ level in Nd^{3+}-doped rare earth gallium nano-garnets. These results indicate that these gallium-based nano-garnets could be an excellent option to replace aluminum-based garnets in photonic and nano-scale applications.

Acknowledgments

Authors are grateful to The Governments of Spain and India for the Indo-Spanish Joint Programme of Bilateral Cooperation in Science and Technology (PRI-PIBIN-2011-1153/DST-INT-Spain-P-38-11). Dr. Venkatramu is grateful to DAE-BRNS, Government of India for the award of DAE Research Award for Young Scientist (No. 2010/20/34/5/BRNS/2223). This work have been partially supported by MINECO under The National Program of Materials (MAT2013-46649-C4-2-P/-3-P/-4-P), The Consolider-Ingenio 2010 Program (MALTA CSD2007-00045), by Fundación CajaCanarias (ENER-01), and by the EU-FEDER funds. V. Monteseguro wishes to thank MICINN for the FPI grant (BES-2011-044596). Authors also thank Agencia Canaria de Investigación, Innovación y Sociedad de la Información for the funds given to Universidad de La Laguna, co-financed by The European Social Fund by a percentage of 85%.